

# RSC Advances



This is an *Accepted Manuscript*, which has been through the Royal Society of Chemistry peer review process and has been accepted for publication.

*Accepted Manuscripts* are published online shortly after acceptance, before technical editing, formatting and proof reading. Using this free service, authors can make their results available to the community, in citable form, before we publish the edited article. This *Accepted Manuscript* will be replaced by the edited, formatted and paginated article as soon as this is available.

You can find more information about *Accepted Manuscripts* in the [Information for Authors](#).

Please note that technical editing may introduce minor changes to the text and/or graphics, which may alter content. The journal's standard [Terms & Conditions](#) and the [Ethical guidelines](#) still apply. In no event shall the Royal Society of Chemistry be held responsible for any errors or omissions in this *Accepted Manuscript* or any consequences arising from the use of any information it contains.

Cite this: DOI: 10.1039/c0xx00000x

www.rsc.org/xxxxxx

PAPER

## Facile synthesis of novel size-controlled antibacterial hybrid sphere with silver nanoparticles loaded to poly-dopamine sphere

Hongyong Luo<sup>a</sup>, Changwei Gu<sup>a</sup>, Weihua Zheng<sup>b</sup>, Fei Dai<sup>a</sup>, Xinling Wang<sup>a</sup>, Zhen Zheng<sup>a\*</sup>*Received (in XXX, XXX) Xth XXXXXXXXX 20XX, Accepted Xth XXXXXXXXX 20XX*

DOI: 10.1039/b000000x

Silver nanoparticles has proven to own excellent antimicrobial activity, but the problems of aggregation and toxicity limit its practical application. To solve the problems, a kind of poly-dopamine sub-micrometer structure-sphere loaded with silver nanoparticles (Ag@PDS) was fabricated by a facile method. Silver nitrate was directly reduced by poly-dopamine sphere without surface modification of the spheres and additional reducing agent. This whole preparation process is very green, simple and time-saving. As a result, Ag NPs have been fixed and uniformly disperse onto the surface of the PDS, which can effectively prevent Ag NPs from aggregation and oxidization in application. Since the size of the uniform hybrid sphere is easily controlled by adjusting the ratio of ammonia to dopamine, it is convenient to fabricate different size hybrid spheres according to need. And the antibacterial activity of this hybrids show that the bacterial growth has fully been inhibited. Finally, prospect of the organismal level impact of the Ag@PDS hybrid has also been proposed.

### Introduction

Antibacterial materials which play critical roles to health care are always widely studied. Silver and antibiotics, to our best knowledge, are two important and popular antibacterial agents. Unfortunately, antibiotics may rise of microbial drug resistance, which results in poor treatment efficacy and significant economic losses.<sup>1</sup> But silver nanoparticles has proven to own excellent antimicrobial activity which is mainly due to the function of deactivating respiratory enzymes and in part by interfering with DNA replication and disrupting the cell membrane.<sup>2</sup> Although the silver nanoparticles has been used in commercial products, it still attract researchers attentions because of its huge practical application and some elusive questions. In recent decades, the effect of silver nanoparticles size, shape, surface charge, solution chemistry, and surface coating to antibacterial properties are widely studied.<sup>3-5</sup> But, the problems of aggregation and oxidization of silver nanoparticles are still the critical factor that exist and limit the practical application through affect the activity of silver nanoparticles.<sup>6</sup> In order to resolve these problems, several novel strategies have been made through preparing silver nano-composites which often synthesizing the silver nanoparticles on the surfaces of nanowires, nanotubes, nanospheres.<sup>7-9</sup> However, it is easy to find that these processes are usually complex. Surface modification of the substrate, additional reductant and multi-steps processes are often needed.

Dopamine has attracted very widespread research interest as a hormone and neurotransmitter in many years.<sup>10, 11</sup> Its unique property of forming coating on various bulk substrates have caused the wide interests of researchers. Once found to easily obtain through self-polymerization process of the dopamine at alkaline conditions, poly-dopamine is quickly applied into various interfaces of different fields, such as the surface modification,<sup>12-16</sup> the enhancement of the electronic properties,<sup>17-20</sup> the biological application,<sup>19-22</sup> and so on. Recently, poly-dopamine sphere (PDS) has been fabricated by a facile method at room temperature.<sup>20</sup> This PDS has many advantages, such as the easily controllable size, uniformly spherical shape, extremely good thermal stability. And the inherit catechol and N-H groups enable yields of transition metal-carbon hybrid materials, which probable greatly enhance its application in the field of electrochemistry. The presence of these functional groups endowed PDS with an active surface for absorbing and reducing metal ions. In addition, this sphere owns huge practical application in the field of biomaterial because of its good biocompatibility and non-toxic property. Due to inherit polar group, it also can disperse in many solvent, which make it used as vector of other poor-dispersion nanoparticles.

In this report, we present a novel kind of uniform hybrid spheres that is PDS loaded with silver nanoparticles (Ag@PDS). This whole preparation process is very facile, simple and time-saving, both surface modification of PDS and additional reductants are not needed (Fig. 1). Specifically, the silver nitrate is directly reduced on the surface of PDS with the assistance of sonication in ice bath. Since the size of the uniform hybrid sphere is easily controlled by adjusting the ratio of ammonia to dopamine, it is convenient to fabricate different size hybrid spheres according to need. In addition, the PDS can well disperse in many solvents, which also results to a well-dispersion of silver nanoparticles because of tight bonding between silver nanoparticles and PDS. Simultaneously, this tight bonding can effectively prevent the aggregation of the silver nanoparticles and possible release of silver ionic. In the hybrid sphere, silver nanoparticles are uniformly distributed on the surface of PDS. This structure has great contribution to the efficient antibacterial activity of Ag@PDS. Moreover, as Ag@PDS has character of good dispersion but poor solubility in solvents, it will dramatically increase its application in the field of antibacterial material by embedding silver nanoparticles into the polymer through solution blending method.

Furthermore, silver nanoparticles (Ag NPs) are increasingly applied in consumer products for their antimicrobial properties and may have adverse impacts on organisms when they enter biotic receptors, though the mechanisms of Ag NP toxicity have not been fully illuminated. In particular, there is debate as to

whether toxicity can be directly attributed either to the nanoparticles themselves or to dissolved ionic silver released from Ag NPs.<sup>23</sup> Liyan Yin's study shows that the release of silver in the form of nanoparticles may be the primary importance compared to the release of ionic Ag from NP.<sup>24</sup> Our silver nanoparticles loaded to poly-dopamine sphere hybrid have high antibacterial property while possesses controllable size of hundreds of nanometers to micrometers, allowing potentially great biocompatibility and possible tailored size effect for antibacterial applications in biotechnology and biomedical fields. Next, in another paper, we discuss that the possibility of the hybrid applied in infected organisms on the premise of reduction of the Ag NPs toxicity due to the hybrid's bigger size and better biocompatibility of dopamine, which will further illustrate the toxicity mechanism of Ag NPs nanoparticles.

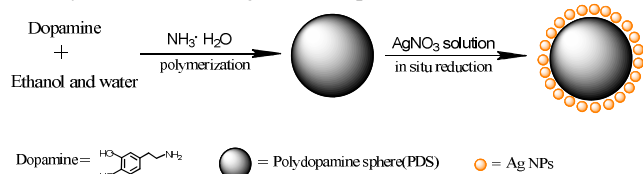


**Fig.1** Schematic illustration of the procedure for fabricating poly-dopamine sub-micrometer sphere loaded with silver nanoparticles (Ag@PDS)

## Experiment

### Material

Dopamine-HCl was purchased from Aladdin-reagent Company without further treatment. Silver nitrate, ethanol and ammonia aqueous solution (25wt%-28wt%) were purchased from Sinopharm Chemical Reagent Co., Ltd. Phosphate buffered saline (PBS) was prepared by dissolving 7.9g NaCl, 0.2g KCl, 0.24g KH<sub>2</sub>PO<sub>4</sub> and 1.44g Na<sub>2</sub>HPO<sub>4</sub> into 800 ml of water. The pH was adjusted to 7.40 with 1 M NaOH or 1 M HCl, and the solution was mixed with additional water to 1 L in a volumetric flask. Bacteria strains *Staphylococcus aureus* (ATCC6538) and *Escherichia coli* (ATCC8739) were purchased from The Shanghai Fu Xiang biological Technology Co., Ltd. Tryptic soy agar was obtained from The Shanghai Zhi Yan biological Technology Co., Ltd.

### Synthesis of poly-dopamine sphere (PDS)

The synthesis is similar to the previous reference.<sup>20</sup> deionized water (90mL) was mixed with ethanol (40mL) at room temperature, ammonia aqueous solution (NH<sub>4</sub>OH, 1mL, 25%) was added into the above solution under mild stirring, then stirred for 30 minutes. Dopamine hydrochloride (0.5 g) was dissolved in deionized water (10mL) and then injected into the above mixture solution. The reaction was allowed to proceed for 30 hours. The PDS were obtained by centrifugation and washed with water for three times. The control over the size of PDS would be achieved by adjusting the amount of ammonia aqueous solution.<sup>20</sup>

### Synthesis of poly-dopamine sphere loaded with silver nanoparticles (Ag@PDS)

The obtained PDS was dispersed in deionized water through stirring and sonication for several minutes, 0.8 g silver nitrate was dissolved in deionized water (10 ml) then dropwise added into the

PDS dispersion, and the reduction reaction carried out for 10min in the ice bath with the assistance of sonication. And the Ag@PDS were collected by centrifugation and washed with deionized water for three times. At last, the products were dried at 60 °C in vacuum for further use.

### Characterization

SEM patterns were all acquired using a scanning electron microscope (JSM-7401F, JEOL) at an acceleration voltage of 5kV. Energy Dispersive Spectrum (EDS) analysis was also performed on the JSM-7401F JEOL instrument during SEM. The morphology of samples were also characterized by transmission electron microscopy (TEM, JEOL, JEM-2100, with an accelerating voltage of 100 kV) equipped with an Oxford INCA Energy TEM 200 EDX system. The particle size distribution were measured using dynamic light scattering (DLS) (Zetasizer ZS, Malvern Instruments Ltd.). The fourier transformed infrared spectroscopies (FTIR) were recorded on a Perkin-Elmer 1000 FTIR spectrometer. The X-ray diffraction (XRD) recorded on Rigaku D/Max 2550 (Cu K $\alpha$ ,  $\lambda=1.5418\text{\AA}$ ) with a 2 $\theta$  scan configuration in the range 5–90°. The surface chemical composition was analyzed using a Shimadzu-Kratos (AXIS Ultra) X-ray photoelectron spectroscopy (XPS).

### Bactericidal testing

#### Inhibition efficiency

The antimicrobial activity of the Ag@PDS was determined using inhibition efficiency and the bactericidal experiment was carried out with the Gram-negative bacteria *Escherichia coli* and the Gram-positive bacteria *Staphylococcus aureus*. A modified AATCC-100 biocidal testing protocol was employed. 100 $\mu\text{L}$  *E. coli* (ATCC8739) or *S. aureus* (ATCC6538) bacteria suspension was grown in 160ml MHB (Mueller-Hinton Broth, cation adjusted) at 37°C for 12h. Then the bacteria containing suspension was diluted 50 times to enable the separate bacterial colonies to be distinctly visible and containing  $\sim 10^6$  CFU mL<sup>-1</sup> colonies. And the algae filament was collected by centrifuge (5000rpm, 10min) from 30 mL of incubated bacteria suspension containing  $\sim 10^6$  CFU mL<sup>-1</sup> colonies, after that 30 mL phosphate buffered saline (PBS) were added to the algae filament. Then 0.15 mg mL<sup>-1</sup> Ag@PDS, PDS, Ag NPs suspension was added to bacteria solution respectively. Each sample contains five repetitions to eliminate accidental factors and get statistical results. Put the suspension into shaker ZHWY-2102C for another 18 h, then 200  $\mu\text{L}$  of final solution was spread out on the plate and incubated at 37 °C for 24 h. The surviving bacteria on the controls and experimental plates were observed.

#### Zone of inhibition (ZOI)

The antimicrobial activities of the Ag@PDS composite spheres were also analyzed by inhibition zone testing. In the inhibition zone test, *S. aureus* bacteria solution was grown in 160ml MHB (Mueller-Hinton Broth, cation adjusted) at 37°C for 12h. Then 200 $\mu\text{L}$  bacteria suspension was uniformly spread over a Luria-Bertani (LB) agar plate. Samples coated with 5mg of Ag@PDS hybrid sphere, PDS, Ag NPs, respectively, and were placed at the center of the agar plate carefully to without touching the other parts and incubated at 37°C for 24 h. Each sample contains five repetitions to eliminate accidental factors and get statistical results. The clear zones in the center of the disks were then photographed and measured with the help of a scale that represented the antibacterial properties of the different composites.

## Results and discussion

### Microstructure and morphology studies

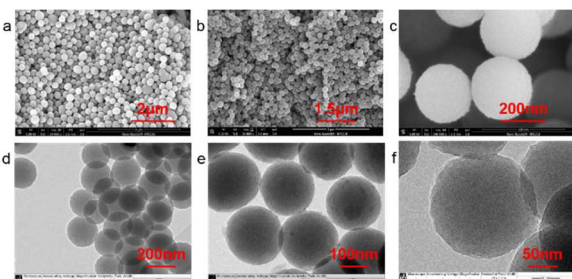


**Fig.2** SEM (a, b, c) and TEM (d, e, f) images of poly-dopamine (PDS) with different scale bars.

At first, uniform PDS were synthesized through a facile process which was carried out at room temperature with gentle stirring (Fig.1). This process takes 30 hours in order to obtain uniform shape spheres.<sup>20</sup> In this study, we found that PDS were available in the solution only after 12 hours and the size was also similar to that of the final products which obtained after 30 hours. But the morphology of the final sphere is much more uniform. And in this synthesized process, the mild stirring plays a key role to obtain uniform spheres. Hundreds of nanometers to micrometers-sized PDS have been successfully synthesized. But the deterioration of dopamine which is easily oxidized probably causes the products of a little different in size (about several to tens nanometers) in the same ratio of ammonia to dopamine under the same experimental condition.

The widespread application of poly-dopamine has also raised the interest of researchers to study the mechanism of dopamine polymerization in recent years (ESI, Fig.S1),<sup>16</sup> but the mechanism, to our best knowledge, has not yet been clearly demonstrated. In this work, we focus on analyzing the structure of PDS. The typical SEM and TEM images of PDS were shown in Fig.2. From the electron microscopy images, it can be clearly found that these organic spheres are uniform. And the diameter of the PDS can be easily controlled by the ratio of ammonia to dopamine.<sup>20</sup> The chemical composition of the sample is determined using the energy dispersive spectrum (SEM-EDS) (ESI, Fig.S2). There are carbon, oxygen, nitrogen and silver elements peaks in the SEM-EDS spectrum taken from Ag@PDS, while there is only carbon and, oxygen and nitrogen peaks taken from PDS. UV-vis measurement (ESI, Fig.S3) shows an absorbance at 280 nm attributed to catechol groups in PDS, which can reduce silver nitrate. The PDS contain several polar groups, such as -OH and C-O, which lead to a very well dispersion in many solvents. Meanwhile, this PDS which is a kind of organic spheres probably possesses a good compatibility in organism, including various biomacromolecules.

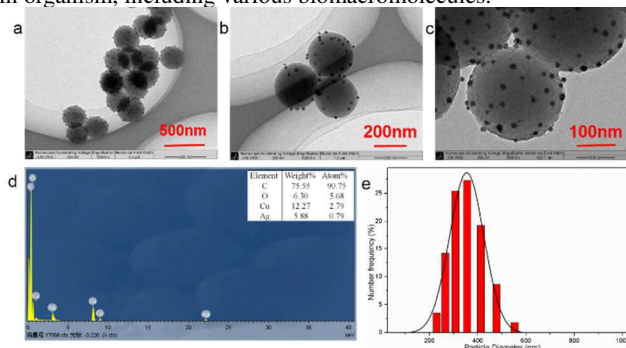


**Fig.3** TEM images (a, b, c) of poly-dopamine sphere loaded with silver nanoparticles (Ag@PDS) with different scale bars, and (d)EDX pattern and (f) DLS curve of Ag@PDS.

In order to obtain the silver nanoparticles loaded to PDS hybrid, we mixed the PDS dispersion with silver nitrate solution in ice bath under sonication. Compared with other reduction process, no additional reductant and heating are needed. Silver nitrate solution was directly reduced to silver nanoparticles because of the catechol groups in the sphere. After reduced, Ag nanoparticles are tightly bonded on to the surface of PDS. So this strategy of getting target products is very simple, facile and environment friendly. TEM images from Fig.3 (a, b, c) show that the silver nanoparticles are successfully attached and uniformly dispersed on the PDS. The size of Ag nanoparticles on the PDS is about 12-18nm, and their shape is spherical. This sphere-structure prevent the aggregation of silver nanoparticles effectively. The chemical composition of the sample is determined using the energy dispersive X-ray spectrum (EDX). As shown in Fig.3d, there are several kinds of peaks in the EDX spectrum taken from the Ag@PDS, which correspond to carbon, oxygen, silver, sulfur and copper elements, respectively. It confirms well the existence of Ag NPs on the surface of the PDS. The elemental atoms results in insert table also confirm that the particles formed on the PDS surface is composed of silver. The dynamic light scattering (DLS) result (Fig.3e) also shows Ag@PDS is about 350nm with narrow size distribution, which corresponds to the size measured by TEM.

Before the measurement of TEM, Ag@PDS was ultrasonicated about 30 minutes, silver nanoparticles were still attached on the PDS and no pure particle was found. It provides evidence that the bonding between silver nanoparticles and PDS is firm and stable. This strong bonding ensures that this nanostructure will not destroy in the process of embedding Ag@PDS into various biomacromolecules. We find that the grow speed of Ag nanoparticles on the PDS is very fast with the assistance of sonication. The time of reaction to obtain the above Ag nanoparticles is only 10 minutes, so this process was rapid and time-saving.

### Crystal forms of Ag@PDS

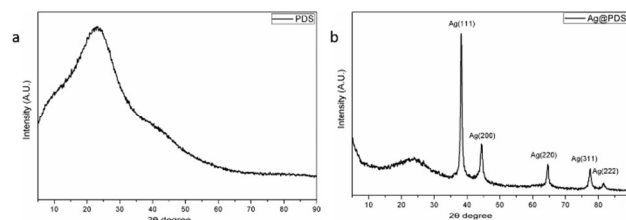


**Fig. 4** XRD patterns of (a) poly-dopamine sphere (PDS) and (b) poly-dopamine sphere loaded with silver nanoparticles (Ag@PDS).

Crystal forms of PDS and Ag@PDS can be identified with XRD patterns (Fig.4). The XRD patterns of the obtained Ag@PDS (Fig.4b) demonstrate the existence of PDS loaded with silver. The broad XRD reflection peak at 23.2° could be attributed to the diffraction of the amorphous structures of the PDS. Five XRD diffraction peaks of Ag@PDS at 2θ of 38.1°, 44.4°, 64.6°, 77.5° and 81.6° correspond to the diffraction of the (111), (200), (220), (311), and (222) lattice planes, indicating a face-centered-cube (FCC) phase of the Ag crystal (JCPDS file no.04-0783), which evidently reveal that silver ions have been reduced to 0 value of metallic and fixed on the surface of PDS. Besides, the peaks belong to amorphous PDS did not change, indicating that the reduction process did not affect the crystallography structure as

well as the good property of the PDS. All of the TEM, EDX and XRD results demonstrated that the AgNPs were successfully synthesized on the PDS surface by this simple facile reduction process.

### 5 FT-IR analysis of Ag@PDS

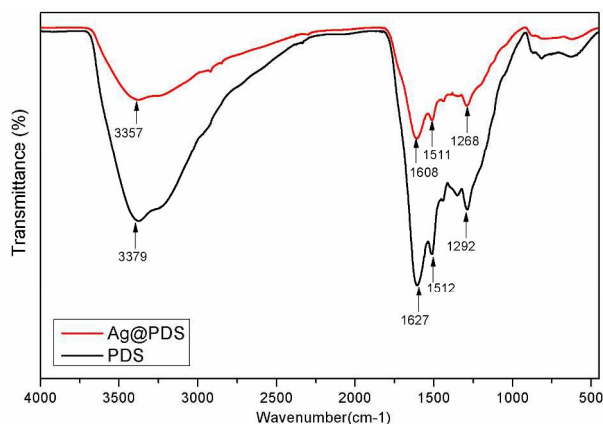


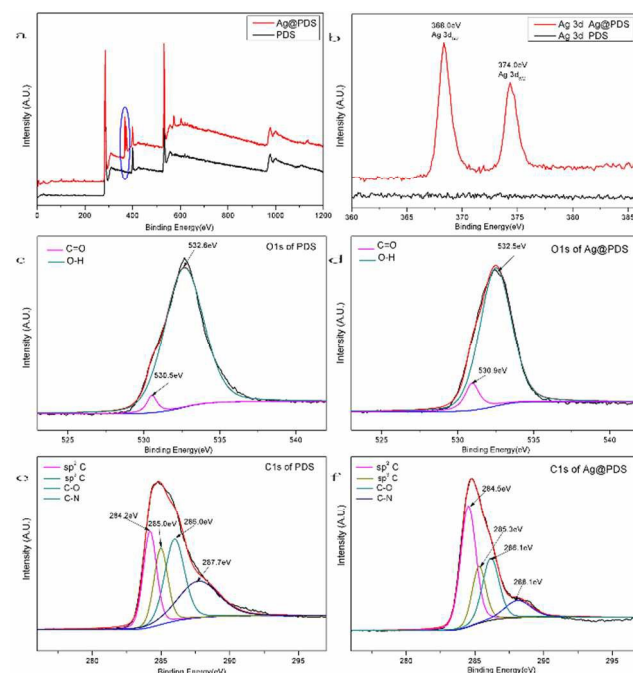
**Fig. 5** FT-IR spectra of poly-dopamine sphere (PDS) and poly-dopamine sphere loaded with silver nanoparticles (Ag@PDS).

FT-IR spectra was chosen to investigate the surface chemical structure of Ag@PDS as well as the binding interactions between PDS and Ag NPs, and the spectra are illustrated in Fig.5. The spectra of the Ag-based samples Ag@PDS display well-defined characteristic bonds that appear also in the spectrum of the PDS but slightly shifted and with difference relative intensity, indicating that the reaction process did not affect the surface chemical structure as well as the good property of the PDS. The absorption band at  $3379\text{ cm}^{-1}$ , which corresponds to the stretching vibrations of  $-\text{OH}$  &  $\text{N}-\text{H}$  groups of PDS, broadened and underwent a low-frequency shift to  $3357\text{ cm}^{-1}$  of Ag@PDS. Such characteristics attributed to the hydrogen bonding between PDS and Ag NPs. Meanwhile, the sharp peak at  $1627\text{ cm}^{-1}$  and  $1292\text{ cm}^{-1}$ , which is attributed to the bond of  $\text{C}=\text{O}$  and  $\text{C}-\text{O}$ , broadened and gradually shifted to lower wavenumbers  $1608\text{ cm}^{-1}$  and  $1268\text{ cm}^{-1}$ . On the other hand, the peak of  $\text{C}=\text{N}$  &  $\text{C}=\text{C}$  at  $1512\text{ cm}^{-1}$  almost stay the same. The peak shifting could be due to bond formation between silver and oxygen, catechol group and hydroxyl group were oxidized to quinone group or carbonyl group while  $\text{Ag}^+$  was reduced to  $\text{Ag}^0$ . The interaction facilitate the attachment of Ag NPs to the PDS surface, leading to the steric stabilization of the particles. Furthermore, the remaining positively charged PDS could prevent the aggregation of Ag NPs by providing reciprocal electrostatic repulsion.

### XPS study of Ag@PDS

To better understand the mechanism underlying the formation of the Ag@PDS, the result was further verified by X-ray photoelectron spectroscopy (XPS) analysis to further illustrate the composition of the PDS and Ag@PDS. Fig.6a shows the XPS wide scan of PDS and Ag@PDS, and high-resolution spectra of Ag 3d, O 1s and C 1s, respectively. The scan survey spectra (Fig.6a) of PDS and Ag@PDS surface showed almost the same peak components of C 1s, N 1s (ESI, Fig.S4) and O 1s.<sup>25</sup> In addition, Ag@PDS exhibited two specific peaks with binding energies of  $368.0\text{ eV}$  and  $374.0\text{ eV}$  in Fig.6b, which were attributed to Ag 3d  $5/2$  and Ag 3d  $3/2$  electrons of  $\text{Ag}^0$ . The spin energy separation was identified as  $6.0\text{ eV}$  which indicates silver on the PDS surface is metallic  $\text{Ag}^0$  in nature; in turn, it further supports the

conclusion that Ag NPs has been successfully loaded to the surface of PDS. The XPS binding energy of the silver is somewhat lower than the values reported by Gole et al.<sup>26</sup> This may be partly from the bonding interaction between Ag NPs and the PDS surface.



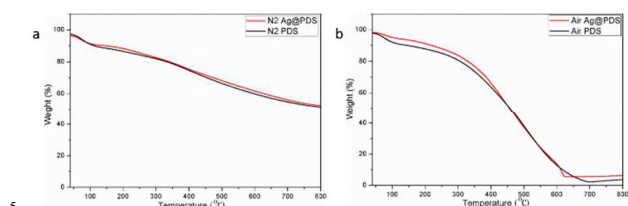
**Fig. 6** X-ray photoelectron spectra (XPS) of (a) scan survey, (b) Ag 3d, (c, d) O 1s, (e, f) C 1s of poly-dopamine sphere (PDS) and poly-dopamine sphere loaded with silver nanoparticles (Ag@PDS).

Fig.6c and Fig.6d show the O 1s high resolution spectrum of PDS and Ag@PDS, with both having two kinds of oxygen species. One peak at  $530.5\text{ eV}$  is closely associated with quinone group or carbonyl group ( $\text{C}=\text{O}$ ) oxygen, while the other peak at  $532.6\text{ eV}$  is attributed to oxygen of surface catechol groups or hydroxyl groups ( $-\text{OH}$ ). It is easily to find some differences from O 1s spectra between PDS and Ag@PDS: After facile stirring process of PDS and  $\text{AgNO}_3$ , the O 1s peak of PDS at  $532.6\text{ eV}$  and  $530.5\text{ eV}$  turned to  $532.5\text{ eV}$  and  $530.9\text{ eV}$  of Ag@PDS. The spin energy separation of Ag@PDS shifts notably to the lower value compared to that of PDS. Besides, the proportion of  $\text{O}-\text{H}/\text{C}=\text{O}$  decreased from  $24.6$  ( $96.1\%/3.9\%$ ) to  $7.9$  ( $87.9\%/11.1\%$ ). These variations should be the results of interaction between the silver with the oxygen functional groups. Oxygen functional groups are the most common functionality in activated carbons and they can adsorb metal ions through ion-exchange reactions. Moreover, only a small amount of energy is required to move atomic oxygen readily through the silver lattice, which makes silver little repulsion to oxygen.<sup>27, 28</sup> The interaction between the AgNPs and supporting PDS will directly lead to the tight adherence of AgNPs to the PDS surface, which is very useful and essential for the practical application.

The C 1s high-resolution spectrum of the PDS (Fig.6e) could be curve-fitted with four peak components, having binding energies at  $284.2\text{ eV}$  for the  $\text{sp}^2\text{C}$  species, at  $285.0\text{ eV}$  for the  $\text{sp}^3\text{C}$  species, at  $286.0\text{ eV}$  for the  $\text{C}-\text{O}$  species, and at  $287.7\text{ eV}$  for the  $\text{C}-\text{N}$  species. The C 1s core-level spectrum of the Ag@PDS (Fig.6f) has almost the same peak components as that of the PDS but the peaks shifted to  $284.5\text{ eV}$ ,  $285.3\text{ eV}$ ,  $286.1\text{ eV}$ ,  $288.1\text{ eV}$ , respectively. The peak for the species of  $\text{C}-\text{O}$  is substantially

decreased, which shows that many oxygen-containing functional groups are reacted or removed due to the interaction of catechol groups with silver.

### Thermal gravity analysis of Ag@PDS



**Fig.7** TGA curves of (a) poly-dopamine sphere (PDS) and (b) poly-dopamine sphere loaded with silver nanoparticles (Ag@PDS).

Thermal Gravity Analysis (TGA) was carried out at the temperature range of 40°C to 800°C to examine the thermal stability of PDA and Ag@PDS. As expected, both PDS and Ag@PDS show excellent thermal stability, 51.6% and 52.5% residual weight of PDS and Ag@PDS were observed even at the end of the analysis (800°C) under N<sub>2</sub> atmosphere, respectively and they exhibits almost the same behavior in Fig 7. While difference of TGA curve can be found under air atmosphere, Ag@PDS show relatively slower rate of weight loss, and it reached balance at 625°C with 6.41% residual weight; while PDS reached balance at a higher temperature of 700°C with 3.06% residual weight.

### Solubility measurement

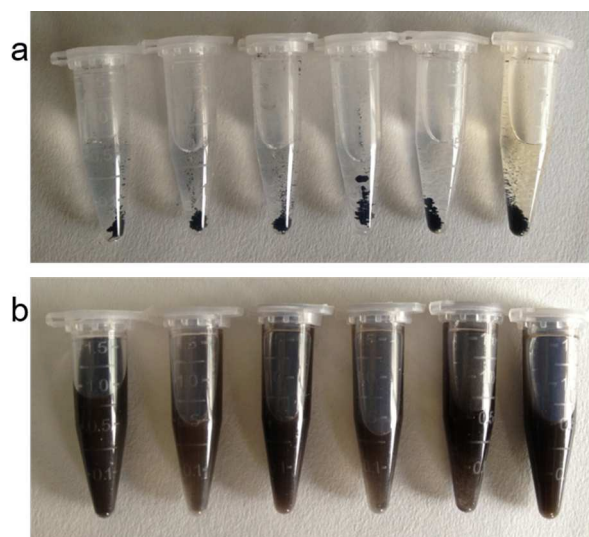


**Fig.8** The images of solubility (a) and dispersion (b) measurement of this poly-dopamine loaded with silver nanoparticles (Ag@PDS) (The solvents from left to right are water, acetone, 1, 4-dioxane, chloroform, toluene, and DMF, respectively).

For the feasibility of application, the solubility and dispersibility of Ag@PDS spheres have been further studied (Fig.8). This experiment demonstrated that several common solvents, such as water, acetone, chloroform, toluene, and N, N-dimethylformamide (DMF), were all can't dissolve these spheres. But due to inherit polar group, PDS owns a perfected dispersion in many solvents after ultrasonic treatment. This characteristic of

good dispersion but poor solubility of the spheres make them perfect vectors for Ag nanoparticles, which will results to uniform and stable dispersion of Ag nanoparticles in the composite through import method of solution blending.

### Antibacterial property

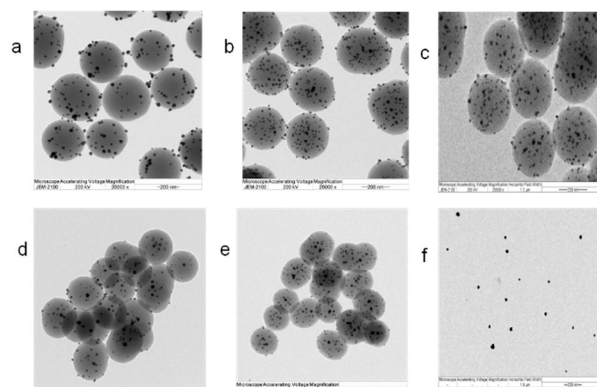


**Fig.9** TEM images with 200nm scale bar of different controllable size of poly-dopamine sphere loaded with silver nanoparticles (Ag@PDS) by adjusting the amount of aqueous ammonium: (a) 1.0ml, (b) 1.25ml, (c) 1.5ml, (d) 1.75ml, (e) 2.0ml and (f) pure Ag NPs. And these Ag@PDS of different size are applied in antibacterial experiment.

Samples designated as Ag@PDS<sub>1.0</sub>, Ag@PDS<sub>1.25</sub>, Ag@PDS<sub>1.5</sub>, Ag@PDS<sub>1.75</sub> and Ag@PDS<sub>2.0</sub> were achieved by adjusting the amount of ammonia aqueous solution with 1.0ml, 1.25ml, 1.5ml, 1.75ml and 2.0ml of ammonia aqueous solution, and keeping the amount of dopamine hydrochloride the same(0.5g). Fig.9 TEM images show that the different sizes of uniform spherical PDS are obtained, and little size PDS is available by adding more ammonia aqueous solution. The diameter of PDS in Ag@PDS<sub>1.0</sub>, Ag@PDS<sub>1.25</sub>, Ag@PDS<sub>1.5</sub>, Ag@PDS<sub>1.75</sub> and Ag@PDS<sub>2.0</sub> are 350nm, 310nm, 280nm, 260nm and 230nm, respectively, while the Ag NPs in these samples are almost the same, mainly 12~18nm. And Ag content measured by TGA are 3.35%, 4.43%, 3.85%, 3.86% and 4.01% for Ag@PDS<sub>1.0</sub>, Ag@PDS<sub>1.25</sub>, Ag@PDS<sub>1.5</sub>, Ag@PDS<sub>1.75</sub> and Ag@PDS<sub>2.0</sub>, respectively. Pure Ag NPs was synthesized according to previous reference<sup>29</sup>, whose size was similar to those Ag NPs on the surface of PDS in Ag@PDS.

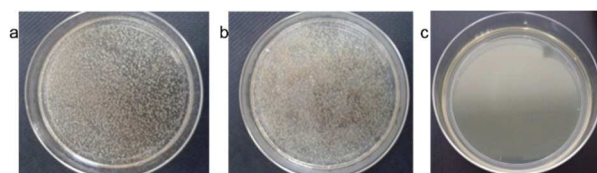


**Fig.10** Images of LB-agar plates which is used in the antibacterial activity experiment of samples against E.coli: (a) control, (b) poly-dopamine (PDS), (c) poly-dopamine sphere loaded with silver nanoparticles (Ag@PDS).

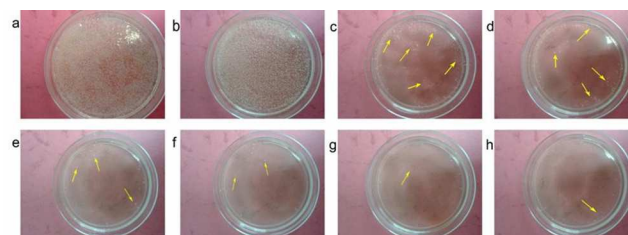


**Fig.11** Antibacteria efficacy of samples against *S.aureus* bacteria. There is a robust growth of bacteria in image (a) and (b), while few surviving bacteria in (c)-(h) samples: (a)control, (b)PDS, (h)pure Ag NPs, (c)-(g) Ag@PDS<sub>x</sub> with different aqueous ammonium amount added: (c) x=1.0ml; (d)x=1.25ml; (e)x=1.5ml; (f)x= 1.75ml; (g)x= 2.0ml.

To investigate the antibacterial activity of our new hybrid material, to our knowledge, which is never been reported, its ability to inhibit Gram-negative bacteria *E. coli* and Gram-positive *S. aureus* bacteria has been measured. Since after the PDS dispersed, the color of LB liquid media became dark, which result impossible to observe the turbidity of the LB liquid media. So the antibacterial efficacy of Ag@PDS was evaluated by the inhibition rate experiment on the LB-agar plates in this report. After the LB-agar plates solidified, the suspension of bacteria was spread onto the LB-agar plates. Then, the above LB-agar plates were cultured at 37°C for 24 h, and the clear evidence which was shown on Fig.10 confirmed that there was a robust growth of *E. coli* bacteria with no samples added. No considerable antibacterial activity was observed in disk with PDS added, indicating that PDS were not toxic to the bacteria. In addition, another controlled experiment which suspension consisted of *E. coli* bacteria and Ag@PDS<sub>2.0</sub> was taken under same condition. Fig.10 shows that few bacteria are observed and this strain is inhibited, which means that this new hybrid material has very strong antimicrobial activity to *E. coli*. In addition, from Fig.11, residual bacteria are fewer with the size of Ag@PDS decreased. Ag@PDS<sub>1.75</sub> and Ag@PDS<sub>2.0</sub> even exhibit fully inhibition of *S.aureus*, and the minimum inhibitory concentration (MIC) against *S.aureus* of Ag@PDS<sub>2.0</sub> is 6μg mL<sup>-1</sup> in Ag content, which is comparable with pure Ag NPs, suggesting that Ag@PDS nanohybrid is an efficient antibacterial material for both Gram-negative and Gram-positive bacteria. This excellent antimicrobial activity has a close relationship with the novel nano-structure which can prevent the agglomeration of the silver nanoparticles, and the large surface area of PDS also provides high load capacity for silver nanoparticles with the assistance of functional groups.

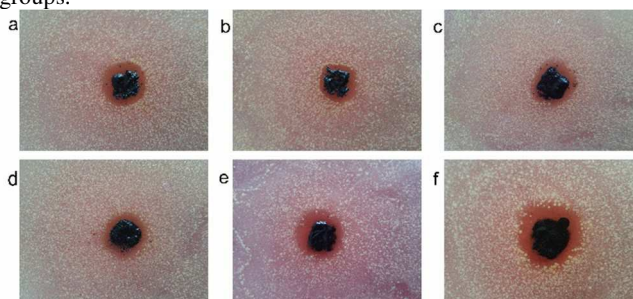


**Fig.12** Disk diffusion tests for different samples against *S.aureus* bacteria. The zone of inhibition (ZOI) appear with an obvious circle indicating a noticeable antibacterial effect. (a)pure Ag NPs, (b)-(f) Ag@PDS<sub>x</sub> with different aqueous ammonium amount added: (b) x=1.0ml; (c)x=1.25ml; (d)x=1.5ml; (e)x= 1.75ml; (f)x= 2.0ml.

To check further the antibacterial effect of Ag@PDS, the Gram-positive representative bacteria *S. aureus* was chosen using the zone of inhibition (ZOI) in a disk diffusion test. The ZOI reflected the magnitude of the susceptibility to the bacteria. It was shown from Fig. 12, clear and significant zone formed against the growth of *S.aureus* in disks with the Ag NPs and Ag@PDS hybrid. The corresponding zone of inhibition (ZOI) are tabulated in Table.1

**Table.1** ZOI value (ratio of ZOI diameter to samples diameter) of samples against *S.aureus* bacteria.

samples	Ag content (μg)	ZOI value (mm/mm)	normalized Ag content (μg)	normalized ZOI value (mm/mm)
PDS	0	-	0	-
Ag NPs	5000	1.81±0.31	200	1.81±0.31
Ag@PDS <sub>1.0</sub>	167.5	1.51±0.33	200	1.50±0.32
Ag@PDS <sub>1.25</sub>	221.5	1.72±0.25	200	1.65±0.23
Ag@PDS <sub>1.5</sub>	192.5	1.75±0.40	200	1.78±0.42
Ag@PDS <sub>1.75</sub>	193	1.83±0.27	200	1.86±0.28
Ag@PDS <sub>2.0</sub>	200.5	1.94±0.33	200	1.94±0.33

It can be seen that the average ZOI values (ratio of ZOI diameter to samples diameter) for the Ag NPs with *S. aureus* was 1.81±0.31, while the corresponding values for Ag@PDS<sub>1.0</sub>, Ag@PDS<sub>1.25</sub>, Ag@PDS<sub>1.5</sub>, Ag@PDS<sub>1.75</sub> and Ag@PDS<sub>2.0</sub> are 1.51±0.33, 1.72±0.25, 1.75±0.40, 1.83±0.27 and 1.94±0.33, respectively. After normalized the Ag concentration to 200μg, the normalized ZOI value of Ag@PDS<sub>1.0</sub>, Ag@PDS<sub>1.25</sub>, Ag@PDS<sub>1.5</sub>, Ag@PDS<sub>1.75</sub> and Ag@PDS<sub>2.0</sub> are 1.50±0.32, 1.65±0.23, 1.78±0.42, 1.86±0.28 and 1.94±0.33, respectively. The specific surface area  $s/m = 4\pi r^2 / (\rho \cdot 4/3 \cdot \pi r^3) = 3 / (\rho \cdot r)$  (unit, m<sup>2</sup>/g) is inversely proportional to the particle size with the same density, it means smaller Ag@PDS has larger specific surface area which contribute to better antibacterial property.

The normalized ZOI value of Ag NPs at normalized Ag content (200μg) turns to 1.03±0.01, which is very unreasonable to the fact that Ag NPs have excellent antibacterial property. According to reference<sup>30</sup>, the antibacterial property of Ag NPs increase with the addition increase, but it is not endless, the antibacterial property of Ag NPs will reach the maximum value and then stay the same with the Ag NPs addition increase to some point (extreme point). The maximum value and the extreme point is limited by the size of Ag NPs, specifically, smaller Ag NPs get higher maximum value and higher extreme point partly due to its larger specific surface area (s/m). So the most probable explanation is that normalized ZOI value of Ag NPs at normalized Ag content (200μg) is the maximum value 1.81±0.31 and it stay unchanged with Ag NPs addition keep increasing to 5000μg. Based on the antibacterial results, we draw the conclusion that the Ag@PDS composites, especially small sized Ag@PDS, have better antibacterial properties in comparison with those of the pure Ag NPs.

According to previous study, the influence of the antibacterial efficiency of Ag NPs might have been derived from the fact that dispersed Ag NPs tend to aggregate and separate from solutions.<sup>6</sup> In our work, Ag NPs have been fixed and uniformly disperse onto the surface of the PDS, which can effectively prevent Ag NPs from aggregation and oxidation in application. Besides, the XPS, FTIR results for the Ag@PDS show surface functional groups such as C-O, O-H which can improve significantly the capacity and dispersion ability of the Ag@PDS. Consequently, the Ag@PDS composites can bind and be in close proximity to the bacterial surface and efficiently inhibited bacteria growth. Therefore, these composites are highly efficient inhibitors of bacterial growth.

## Conclusion

We presented a novel micro-structure which composed of uniformly PDS and Ag nanoparticles. PDS as a carrier in this structure effectively prevent agglomeration of Ag nanoparticles, and its antibacterial activity has been firstly studied in the report.

This whole preparation process is very facile, simple, green and time-saving, both surface modification of PDS and additional reductants are not needed. In the hybrid sphere, silver nanoparticles are uniformly distributed on the surface of PDS, which prevent the aggregation of the silver nanoparticles effectively. And this hybrid material has high antibacterial activity. Because of the PDS's good compatibility in the substrates, it will contribute a lot to the stable and uniform distribution of silver nanoparticles in various media. This will increase dramatically the antibacterial application of this hybrid sphere in biotechnology and biomedical fields. In addition, our silver nanoparticles loaded to poly-dopamine sphere hybrid have high antibacterial property while possesses controllable size of hundreds of nanometers to micrometers, which makes its application in biomedical fields possible for reducing the Ag NPs toxicity, and further provides some support to illustrate the toxicity mechanism of Ag nanoparticles.

### Acknowledge

This project is supported by the National Science Fund of China (20974061) and the Shanghai Leading Academic Discipline Project (No. B202). We thank Dr. Limin Sun from Instrumental Analysis Center of Shanghai Jiao Tong University for his assistance in the XPS experiments.

### Notes and references

<sup>a</sup> School of Chemical and Chemical Engineering, Shanghai Jiao Tong University, 800 Dongchuan Road, Minghang District, Shanghai, P. R. China. Fax: +86 21-54741297; Tel: +86 21-54745817; E-mail: zzheng@sjtu.edu.cn.

<sup>b</sup> Serionix Inc. Champaign IL, 61820, USA

- 1 J. Tang , Q. Chen , L. G. Xu , S. Zhang ,L. Z. Feng , L. Cheng , H. Xu , Z. Liu , and R. Peng, ACS Appl. Mater. Interface., 2013, 5, 3867–3874.
- 2 J. S. Lee and W. L. Murphy, Advanced Materials., 2013, 8, 1173–1179.
- 3 Z. M. Xiu, Q. B. Zhang, H. L. Puppala , V. L. Colvin, and P. J. J. Alvarez, Nano Lett., 2012, 12, 4271–4275.
- 4 Carlson, C. Hussain, S. M. Schrand, A. M. Braydich-Stolle, L. K. Hess, K. L. Jones and R. L. Schlager, J. Phys. Chem. B., 2008, 112–117.
- 5 Yang, X. Y. Gondikas, A. P. Marinakos, S. M. Auffan, M. Liu, J. Hsu-Kim and H. Meyer, J. N. Environ. Sci. Technol. 2012, 46 (2), 1119–1127.
- 6 Z. Zhang, J. Zhang, B. Zhang and J. Tang, Nanoscale., 2013, 5, 118–123 .
- 7 M. Lv, S. Su, Y. He, Q. Huang, W. B. Hu, D. Li, C. H. Fan and S. T. Lee, Adv. Mater., 2010, 22, 5463–5467.
- 8 P. Gunawan, C. Guan, X. H. Song, Q. Y. Zhang, S. S. J. Leong, C. Y. Tang, Y. Chen, M. B. Chan-Park, M. W. Chang, K. A. Wang and R. Xu, ACS Nano., 2011, 5, 10033–10040.
- 9 J. H. Cui, C. F. Hu, Y. H. Yang, Y. J. Wu, L. F. Yang, Y. L. Wang, Y. L. Liu and Z. Y. Jiang, J. Mater. Chem., 2012, 22, 8121–8126.
- 10 R. M. Wightman, L. J. May and A. C. Michael, Anal. Chem., 1988, 60, 769–775.
- 11 A. Zhang, J. L. Neumeyer and R. J. Baldessarini, Chem. Rev., 2007, 107, 274–278.
- 12 L. Wang, D. Wang, Z. H. Dong, F. X. Zhang and J. Jin, Nano Lett., 2013, 13 (4), 1711–1716.
- 13 J. H. Kong, W. A. Yee, L. P. Yang, Y. F. Wei, S. L. Phua, H. G. Ong, J. M. Ang, X. Li and X. H. Lu, Chem. Commun., 2012, 48, 10316–10318.
- 14 H. Jiang, L.P. Yang, C. Z. Li, C.Y. Yan, P. S. Lee and J. Ma, Energy Environ. Sci., 2011, 4, 1813–1821.
- 15 M. H. Ryou, Y. M. Lee, J. K. Park and J. W. Choi, Advanced Materials., 2011, 27, 3066–3070.

- 16 N. F. D. Vecchia, R. Avolio, M. Alfè, M. E. Errico, A. Napolitano and M. d'Ischia\*, Adv. Funct. Mater., 2013, 23, 1331–1340.
- 17 S. M. Kang, I. You, W. K. Cho, H. K. Shon, T. G. Lee, I. S. Choi, J. M. Karp and H. Lee., Angew. Chem. Int. Ed., 2010, 49, 9401–9404.
- 18 S.L. Phua , L. Yang , C. L. Toh , G. Q. Du, S.K Lau , A . Dasari and X. Lu, ACS Appl Mater Interfaces., 2013 , 5, 1302–1309.
- 19 D. E. Fullenkamp, J. G . Rivera , Y. K. Gong , K. H. Lau , L. He, R. Varshney and P. B. Messersmith., Biomaterials., 2012, 33, 3783–3791.
- 20 K. Ai, Y. L. Liu<sup>1</sup>, C. P. Ruan<sup>1</sup>, L. H. Lu and G. Q. Lu, Advanced Materials., 2013, 7, 998–1003.
- 21 L. Zhang , J. J. Wu , Y. X. Wang , Y. H. Long , N. Zhao and Jian Xu, J. Am. Chem. Soc., 2012, 134, 9879 – 9881.
- 22 J. W. Cui, Y. J. Wang, A. Postma, J. C. Hao, L. H. Rigau and F. Caruso, Advanced Functional Materials., 2010,10,1625–1631.
- 23 C. M. Jones and Eric M. V. Hoek, J Nanopart Res., 2010, 12, 1531–1551.
- 24 L. Y. Yin, Y. W. Cheng, B. Espinasse, B. P. Colman, M. Auffan, M. Wiesner, J. Rose, J. Liu, and E. S. Bernhardt, Environ. Sci. Technol., 2011, 45, 2360–2367.
- 25 J. F. Moulder, W. F. Stickle, P. E. Sobol, K. D. Bomben, Handbook of X-ray Photo electronspectroscopy: A reference Book of Standard Spectra for identification and Interpretation of XPS Data, Physical Electronics, Reissue edition, Physical Electronics, USA 18725, Lakedrive East, Chanhassen, MN 55317, 1992.
- 26 A. Gole, S. R. Sainkar and M. Sastry, Chem. Mater., 2000, 12, 1234–1239.
- 27 R. A. Outlaw and M. R. Davidson, J. Vac. Sci. Technol., A, 1994,12, 854–860.
- 28 M. E. Eberhart, M. M. Donovan and R. A. Outlaw, Phys. Rev. B: Condens. Matter, 1992, 46, 12744–12747.
- 29 J. H. Cui, C. F. Hu, Y. H. Yang, Y. J. Wu, L. F. Yang, Y. L. Wang, Y. L. Liu and Z. Y. Jiang, J. Mater. Chem., 2012, 22, 8121–8126.
- 30 S. Agnihotri, S. Mukherjin and S. Mukherj, RSC Adv, 2014, 4, 3974–3983.

# Facile synthesis of novel size-controlled antibacterial hybrid sphere with silver nanoparticles loaded to poly-dopamine sphere

Hongyong Luo, Changwei Gu, Xinling Wang, Zhen Zheng\*

School of Chemistry and Chemical Engineering, Shanghai Jiao Tong University, 800 Dongchuan Road, Shanghai 200240, P.R.China.

E-mail: zzheng@sjtu.edu.cn; Fax: +86 21 54741297; Tel: +86 21 54745817

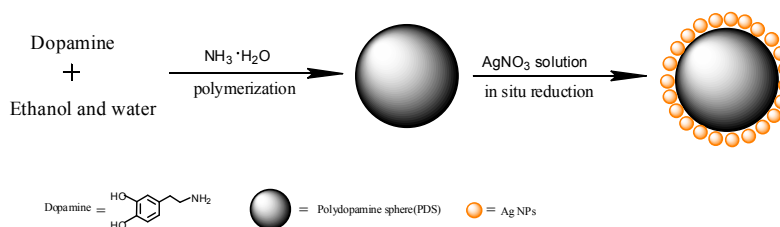


**Fig.1** Schematic illustration of the procedure for fabricating poly-dopamine sub-micrometer sphere loaded with silver nanoparticles (Ag@PDS).

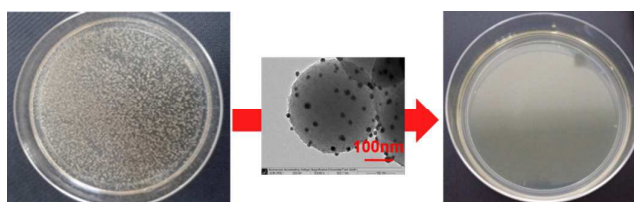


**Fig.2** Antibacterial result of poly-dopamine sub-micrometer sphere loaded with silver nanoparticles (Ag@PDS)

Sub-micrometer structure hybrid spheres with poly-dopamine core and silver-particles embellishment was fabricated by a facile method. This new hybrid sphere owns strong antibacterial activity because of the special structure effectively prevents the aggregation of silver nanoparticles.

## Abstract

Silver nanoparticles has proven to own excellent antimicrobial activity, but the problems of aggregation and toxicity limit its practical application. To solve the problems, a kind of poly-dopamine sub-micrometer structure-sphere loaded with silver nanoparticles (Ag@PDS) was fabricated by a facile method. Silver nitrate was directly reduced by poly-dopamine sphere without surface modification of the spheres and additional reducing agent. This whole preparation process is very green, simple and time-saving. As a result, Ag NPs have been fixed and uniformly disperse onto the surface of the PDS, which can effectively prevent Ag NPs from aggregation and oxidization in application. Since the size of the uniform hybrid sphere is easily controlled by adjusting the ratio of ammonia to dopamine, it is convenient to fabricate different size hybrid spheres according to need. And the antibacterial activity of this hybrids show that the bacterial growth has fully been inhibited. Finally, prospect of the organismal level impact of the Ag@PDS hybrid has also been proposed.